Tethys
Journal of Mediterranean Meteorology & Climatology

Tethys 2012, **9**, 43–51
www.tethys.cat
ISSN-1697-1523
eISSN-1139-3394
DOI:10.3369/tethys.2012.9.05
Journal edited by **ACAM**

Atmospheric surface layer in a coastal environment: measurements in a 100 m tower (El Arenosillo)

J. A. Adame[1], I. Bamberger[2], M. A. Hernández-Ceballos[1] and B. De la Morena[2]

[1]Atmospheric Sounding Station "El Arenosillo, Atmospheric Research and Instrumentation Branch, National Institute for Aerospace Technology (INTA), Mazagón-Huelva

[2]Department of Applied Physics, Facultad de Ciencias Experimentales, Universidad de Huelva, Huelva

Received: 1-V-2012 – Accepted: 3-X-2012 – **Translated version**

Correspondence to: adamecj@inta.es

Abstract

In the southwest of the Iberian Peninsula there is a 100 m high tower, equipped with meteorological instrumentation at the 10, 50 and 100 m levels. The first observations of temperature, relative humidity, wind (direction and speed) and pressure were recorded in 2009. From the original data with a 10-minute resolution, hourly values were calculated applying quality criteria. Using these values, we have obtained various statistical parameters such as percentiles, maxima and minima. The wind regime has also been analyzed. The first 100 m of the atmosphere show an increase in temperature with height, which could be associated with the frequent occurrence of stably stratified conditions. By contrast, the relative humidity has a slight trend to decrease or maintain similar values. As expected, pressure values show a trend to decrease with height. Wind data show flows with similar directions at the three heights and an increase in wind speed. The daily evolution of the atmospheric stratification stability has been estimated using the potential temperature and its difference between levels. As a daily average, in summer the day can be divided into 12 hours of vertical mixing, and thermal inversion for the other 12. In the colder months, 15 hours of stably stratified stability were found. Finally, we have analyzed specific periods, which represent the typical meteorological scenarios of this region, governed by both synoptic and mesoscale processes. In these cases, the stability of atmospheric stratification has been estimated using potential temperature and the Bulk Richardson Number. Under breeze or NE flow conditions, we obtain a daily pattern of atmospheric stratification stability strongly influenced by daytime heating and nighttime cooling, similar to the behavior shown by the planetary boundary layer. However, under SW-W or NW flows, the daily evolution of the potential temperature difference and the Bulk Richardson Number does not present a clear daily cycle, which could be attributed to the influence of the marine boundary layer.

Key words: atmospheric boundary layer, atmospheric stratification stability, potential temperature, Bulk Richardson Number, tall towers

1 Introduction

Due to the progressive and growing need for a greater amount of meteorological information that may give an effective response to the two biggest problems to be faced by humanity in coming years, air quality and climate change (IPCC, 2007), there is now a large, varied set of observational networks that provide information about the state of the atmosphere.

The observations recorded in these observational networks provide information on the physical and chemical processes that occur in the lowest layers of the atmosphere. This information is supplemented by the behavior of the vertical structure, conducting meteorological surveys, using airborne platforms (Heue et al., 2010) or collecting data from satellites (Antón et al., 2010).

However, in the last decades, other types of platforms have begun to be used, such as those known as tall towers.

These are generally platforms over 50 m high, which have the advantage of being able to provide continuous data on different levels of the lower atmosphere, which can increase the degree of vertical representation of the parameters analyzed.

At present there are networks of tall towers for monitoring the atmosphere in both the US and Europe. In the United States there is a network of nine towers located throughout the country, belonging to the National Oceanic and Atmospheric Administration Earth System Research Laboratory Global Monitoring Division (NOAA ESRL/GMD), used to monitor chemical and meteorological parameters. Studies on climate change, air quality and the dynamics of the atmospheric boundary layer have been conducted using it.

In Europe there is a network of tall towers called Tall Tower and surface Observation Research network for verification of Climate relevant emissions of Human origin in Europe (TTORCH), the aim of which is to obtain different measurements on several greenhouse gases (CH_4, N_2O, SF_6) and trace substances (such as CO, H_2, $^{14}CO_2$). A network of towers has also been used in recent years for measuring gases directly related to the carbon cycle called ICOS (Integrated Carbon Observing System - http://www.icos-infrastructure.eu). As a reference and example of tall towers in Europe, we would mention the Cabauw tower (the Netherlands), which is more than 213 m, that was first used in the 1970s to study the atmospheric boundary layer (Wehner et al., 2010; Zieger et al., 2010).

On the Iberian Peninsula (hereafter IP) there are very few such towers, and there is only one in the TTORCH network, located in the northeast. There is a 100 m tower in the northern IP, which belongs to the Centre for Low Atmosphere Research of the University of Valladolid and the Spanish Meteorological Agency, where studies of the atmospheric boundary layer are conducted (Cuxart et al., 2000; Vindel et al., 2008).

The only tower in the center and south of the peninsula is located at El Arenosillo, thus being the only research platform of this kind. In late 2008, the Atmospheric Sounding Station at El Arenosillo, belonging to the National Institute for Aerospace Technology (INTA), installed three meteorological sensors at 10, 50 and 100 m levels in the tower. Therefore, since then, there has been continuous weather information available concerning the behavior of different meteorological parameters in the more superficial layers of the atmosphere.

This weather information has been used for the interpretation of high radon concentrations (Grossi et al., 2010, 2012) and, in 2008, in the analysis of different atmospheric compounds: gases (O_3, NO, NO_2, SO_2, HONO, N_2O_5, NO_3) and radicals (OH, HO_2, RO_2, OH reactivity, etc.) measured during the DOMINO campaign (Diel Oxidant Mechanism in relation to Nitrogen Oxides) (Song et al., 2011; Sinha et al., 2012).

However, this ongoing information has not yet been used in the characterization of the Atmospheric Surface Layer - ASL. This is the thinner atmospheric layer, the closest to the ground, and the turbulent fluxes in it vary less than 10% of their value on the land surface. The study of this layer is of particular importance, since abrupt changes of weather variables with height happen in it, as well as most exchanges of heat, mass and momentum from the atmosphere to the ground from turbulent motions.

Therefore, the aim of this work, based on the analysis of the database in 2009, is to analyze the evolution and behavior of a series of atmospheric variables (temperature, humidity, wind and pressure) and stability parameters (potential temperature gradient and Bulk Richardson Number) that allow the behavior of the ASL in this coastal environment of Southwest IP to be characterized.

2 Study region, data and methodology

2.1 Study Area

The 100 m tower is in the facilities of the experimentation center "El Arenosillo" (CEDEA) (37,1°N, 6,7°W, 42 m above sea level (asl)), belonging to the National Institute for Aerospace Technology (INTA), which is located in the southwest of the IP, 35 km south-east of the city of Huelva (Figure 1). The site is surrounded by a pine forest in Doñana National Park. The 100 m tower is located about 450 meters from the shoreline, in a flat area under 100 m above sea level, which remains homogeneous for a radius of more than 20 km.

2.2 Meteorological information processing

The three sensors placed in the tower at 10, 50 and 100 m are Vaisala WTX520 sensors. These allow the measuring of temperature, air pressure, relative humidity, wind speed and direction. The instrument measures air temperature, barometric pressure and relative humidity with three different sensors. The measurement principle is based on an RC oscillator (resistor/capacitor) and two reference capacitors. To measure the temperature, a ceramic thermal capacitor is used, a silicon capacitive sensor and a pressure sensor with a capacitive thin polymer film for humidity. The working range for temperature goes from -52°C to 60°C with an accuracy of 0.3°C, for pressure it ranges from 600 to 1100 hPa with an accuracy of 0.5 hPa, and for moisture it goes from 0 to 100% with 0.1% accuracy. To measure the wind speed and direction a sensor is used, which has a working range of 0 to 60 m s^{-1} and an accuracy of 0.3 m s^{-1} in the case of speed, and 0 to 360° and 1° accuracy in the case of direction. A system for storing information is located at the tower base, which is sent to a data server via radio.

The measurement period used in this work runs from 1 January to 31 December 2009. The original data was obtained as 10 minute averages. The hourly averages were calculated from these records; to do this, the quality criteria were applied based on the necessary existence of 75% of 10-minute data for the calculation of the corresponding hourly

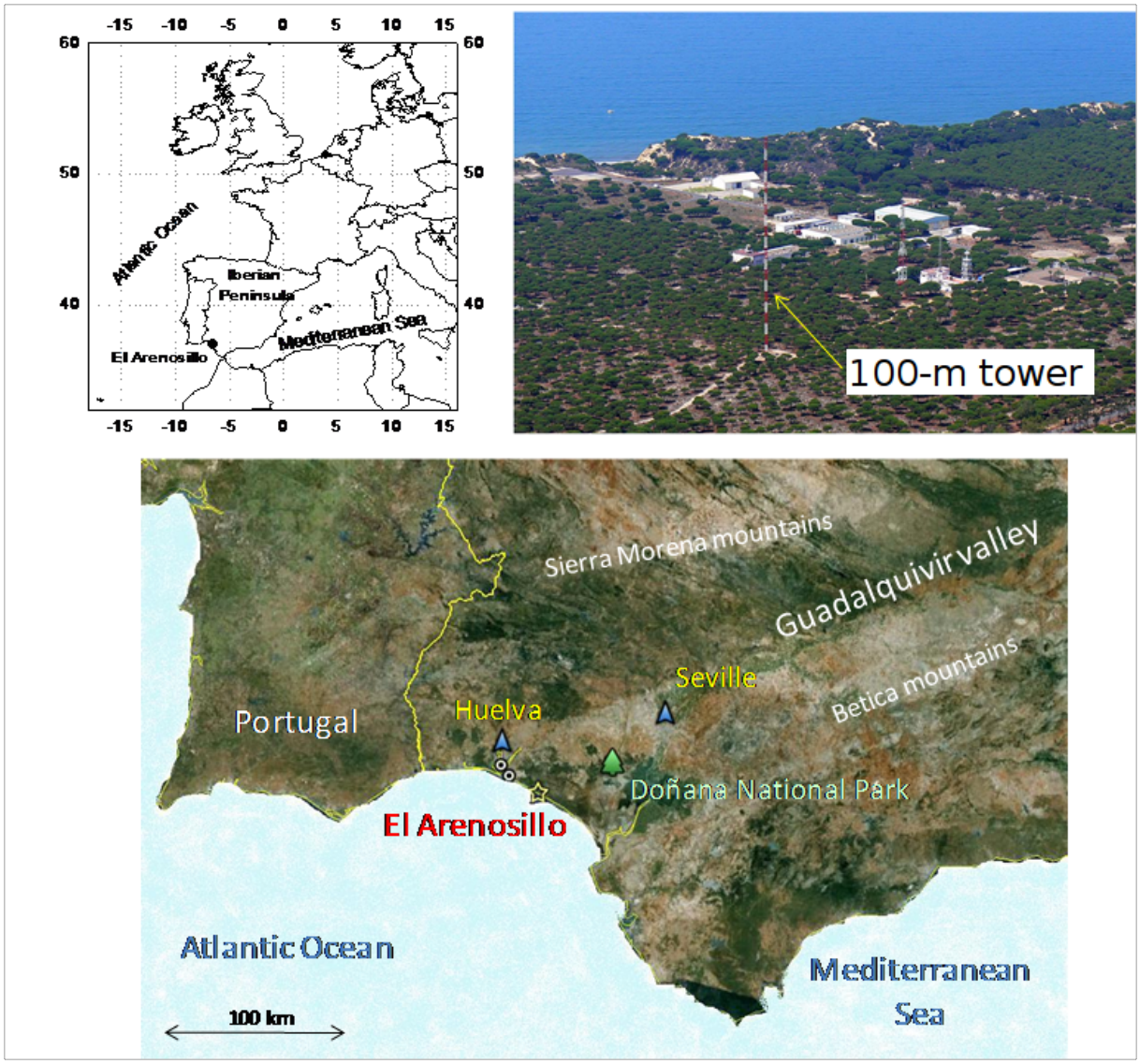

Figure 1. Location of the study area and position of the 100 m meteorological tower.

value. After obtaining the hourly values, all values of the studied annual period were plotted and displayed in order to identify possible anomalous values.

2.3 Experimental estimation of stratification stability

Atmospheric stratification stability is a concept associated with the vertical movements occurring in the atmosphere, thus defining the degree of atmospheric stratification stability from the temperature difference between a portion of air and the surrounding air. In the case of an atmospheric situation with stably stratified stability, the inhibition of the vertical movement of the air portion occurs, while an unstable stratified situation promotes this vertical displacement. Thus, the stability stratification states of the lower troposphere determine the daily evolution of the thickness of the boundary layer, as well as its sub-layers, such as the surface layer. This layer is in contact with the ground surface and high gradients of temperature, humidity and wind velocity take place in it (Stull, 1988; Crespí, 2002). Wind direction suffers no major changes and the Coriolis Effect is not significant. The depth of this layer is approximately 10% of the atmospheric boundary layer.

From the meteorological records at different heights provided by the sensors on the tower, we can estimate the degree of stability of atmospheric stratification between them. In this work, we have conducted this study from the calculation and analysis of the vertical gradient of potential temperature, as well as the Bulk Richardson Number (Oncley et al., 1996; Arya, 2001) (Table 1).

Table 1. Expressions for the calculation of atmospheric stratification stability, where P_0 = 1000 hPa, P is the pressure of the analyzed stratus and $\kappa = \frac{R_d}{cp}$ (0.286), R is the constant of the ideal gases (dry air), cp is the specific heat of the air at constant pressure, g the gravity (9.81 m s^{-2}), z_1 and z_2 the height of the considered stratum, T_0 the average temperature between both, $\Delta\Theta$ is the difference of potential temperature Θ and ΔU the difference of wind speed.

	Stable	Neutral	Unstable		
Potential temperature	$\frac{\partial\Theta}{\partial z} > 0$	$\frac{\partial\Theta}{\partial z} = 0$	$\frac{\partial\Theta}{\partial z} < 0$	where	$\Theta = T\left(\frac{P_0}{P}\right)^{\kappa}$
Bulk Richardson Number	$R_b > 0$	$R_b = 0$	$R_b > 0$	where	$R_b = \frac{\frac{g}{T_0}\sqrt{z_1 z_2}\ln\left(\frac{z_2}{z_1}\right)\Delta\Theta}{\Delta U^2}$

Table 2. Yearly statistic (D as availability in percentage; Max as maximum; percentiles 95, 75, 50, 25, 5 as P95, P75, P50, P25, P5, average and its deviation as M$\pm\ \sigma$ and minimum as Min) of the temperature hourly series (T) in °C, relative humidity (HR) in %, atmospheric pressure (P) in hPa for the 10-, 50- and 100 m levels.

	Parameter	D	Max	P95	P75	P50	M$\pm\ \sigma$	P25	P5	Min
	T10	99	33.7	27.4	21.9	17.3	17$\pm$ 6	13.2	7.8	-2.2
T	T50	83	31.4	26.4	22.1	18.0	18$\pm$ 5	13.8	9.4	2.1
	T100	68	33.0	27.3	22.7	19.0	18$\pm$ 6	13.9	9.5	3.3
	HR10	99	93	90	81	69	67$\pm$ 16	56	37	14
HR	HR50	83	100	92	80	69	67$\pm$ 16	56	38	13
	HR100	68	100	92	78	65	64$\pm$ 18	49	33	12
	P10	99	1026	1017	1013	1010	1010$\pm$ 5	1008	1000	978
P	P50	83	1022	1013	1009	1006	1006$\pm$ 5	1004	999	974
	P100	68	1013	1007	1003	1001	1001$\pm$ 4	999	994	969

3 Results

3.1 Statistical analysis

In order to display the values of the meteorological variables measured in the three levels during the study period, a set of statistical parameters, based on hourly values, was calculated. Table 2 shows the annual mean values with their corresponding standard deviation, absolute maxima and minima and percentiles, 75, 50 (median), 25 and 5 of temperature, relative humidity and pressure at all three levels.

These values have been calculated from a high availability of hourly data, which are also shown in Table 2. Thus, at the 10 m level there is 99% availability, 83% at the 50 m level, and finally 63% at 100 m, because there is less time coverage during the fall and winter.

The temperature shows an average value of 17°C at the 10 m level, and 18°C, at 50 m and 100 m, with a standard deviation of 5-6°C. Six of the eight parameters analyzed for temperature have a trend to increase with height, with the highest values recorded at the 100 m level. However, at this level the data loss is larger due to technical problems. Considering the first 50 meters (values of 10 and 50 m) and those parameters in which there is an increase of temperature with altitude, the gradient ranges from 0.2°C (for percentile 75) and 4.3°C (for minimum). The trend observed is that the lower the temperature values, the larger the differences. These results indicate a stably stratified stability of the atmosphere in its first meters. This site would be subjected to weather scenarios where stably stratified conditions do not always happen. However, the results obtained using one year of data reflect that the most frequent situation would be stably layered stability.

The average relative humidity values are very similar, with average values of 67% at the 10 and 50 m levels, and 64% at 100 m. Except for the maximum and 95th percentile, the other statistics show a slight decrease with height, or even the same values. Considering the first 50 meters, as at 100 m there is a lower percentage of valid data, the decrease is either zero or 1%. Therefore, this parameter in general, considering this annual series, practically maintains its values in the first few meters of the atmosphere.

The pressure shows a clear tendency to decrease with height for all selected statistics, with differences ranging in the first 100 m between 6 and 13 hPa. The largest decrease was obtained for the absolute maximum, while the smallest decrease was found in the 5th percentile. Wind analysis was performed with the calculation of annual wind roses at all three levels (Figure 2). A similar wind behavior was obtained at the three heights, prevailing winds from the third and fourth quadrant, mainly from the west (W) and north (N). Also, there was an increase of speed with height, with the strongest values recorded at the 100 m level, where winds from the W predominate.

This predominance of winds from the W and N in 2009 showed some differences to those obtained from the historical series. In this area of the IP, the wind regime is a combination of both the development of local winds, of mesoscale origin, and the arrival of synoptic winds. Previous studies

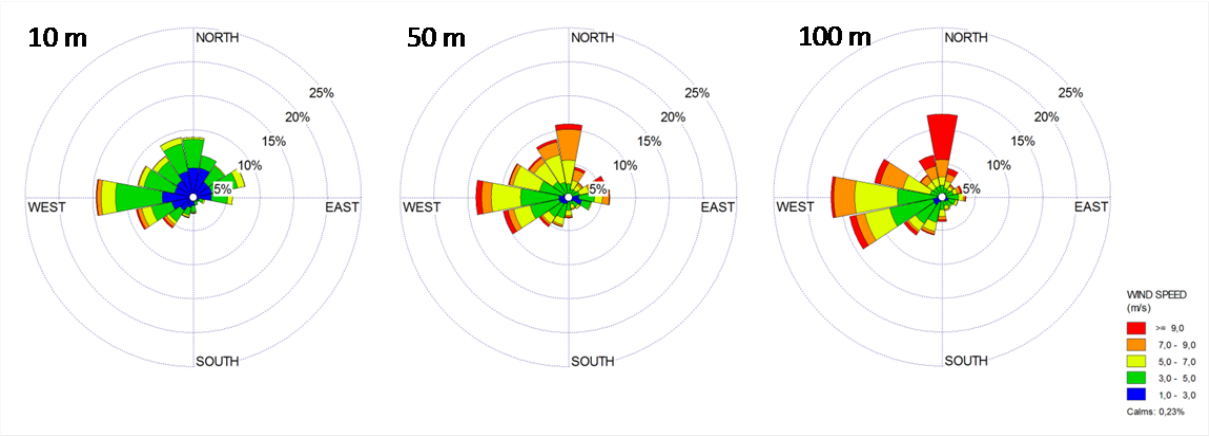

Figure 2. Yearly wind roses at 10, 50 and 100 m from wind hourly values.

show that local scale winds are the cause of the flows detected from the SW, NW and NE, as a result of the coast orientation and the sea breeze development. Two patterns of coastal breeze have been identified in this region, one of them called pure and another one, with synoptic forcing, known as non pure (Adame et al., 2010a). The day regime of both patterns is similar, with winds blowing from the sea, heading SW. However, the night regime in pure breeze blows from the NE, and from the NW for the non pure, while the prevailing synoptic winds come from the first and third quadrant (Adame et al., 2010b). Air masses from northern Europe and the North Atlantic cross the IP and are the origin of those from the NE. The third quadrant flows are caused by anticyclonic situations, which are common in summer or in low pressures, more likely in the colder months.

The seasonal analysis of wind patterns shows that in 2009 the highest prevalence of anticyclone situations in the warmer months favored higher frequency winds from the NW and WSW, while the scarce arrival of winds from the NE could be associated to a lower arrival of air masses from the center of the IP and/or Europe, in the case of synoptic origin; or to a lower development of typical coastal breezes, with nocturnal flows perpendicular to the shoreline, in the case of those of mesoscale origin.

3.2 Daily variation of potential temperature. Estimation of the atmospheric stratification stability

An estimation of the atmospheric stratification stability can be made from the vertical variation experienced by potential temperature (Θ). This section presents the average daily change of this variable for the four seasons, in order to estimate the stability of atmospheric stratification in the boundary layer throughout the year. Due to the reduced availability of hourly data during the fall at the 100 m level, these data have not been used.

The results of the seasonal variation of the potential temperature and the respective differences between each of the levels (highest level minus lowest level) show an increase of this variable during the warmer months of the year, and a widening gap between levels during the spring and summer (Figure 3). In other words, in the cold months the thermal contrast is less than in the warmer months.

Ordered from high to low, we get the differences in potential temperature in summer, fall, spring, and winter. Between the levels, the largest differences were obtained between 10 and 100 m, 10 and 50 m; while the smallest differences were found between 50 and 100 m. Furthermore, the differences found when using the 10 m data, both with 50 and 100 m, were larger than if only using 50 and 100 m. In summer, for example, differences close to 3°C were observed between 10 and 100 m, while between 50 and 100 m these were less than 0.5°C between 6:00 and 18:00 UTC. In other words, the temperature gradient obtained between 10 and 50 m was higher than between 50 and 100 m. These results reflect a higher cooling/heating in the first meters of the atmosphere, whereas above 50 m, the thermal conditions may be more homogeneous.

There are two distinct periods motivated by the sign of their differences. While negative differences (unstably stratified) occur in summer from 6:00 to 18:00 UTC, in winter they take place between 9:00 and 18:00 UTC. These results could indicate that vertical mixing processes can happen for three more hours in summer (12 hours) than in winter (9 hours). The origin could be due to a lower heating of the surface layer during the day in the winter months and result in a longer duration of the temperature inversion. By contrast, in summer the temperature inversion is shorter, the warming is greater due to more radiation and sunshine hours, which also causes a greater temperature difference between heights.

3.3 Estimation of stable stratification in different weather scenarios

As previously mentioned, the SW of the IP is under meteorological processes of synoptic origin with flows mainly

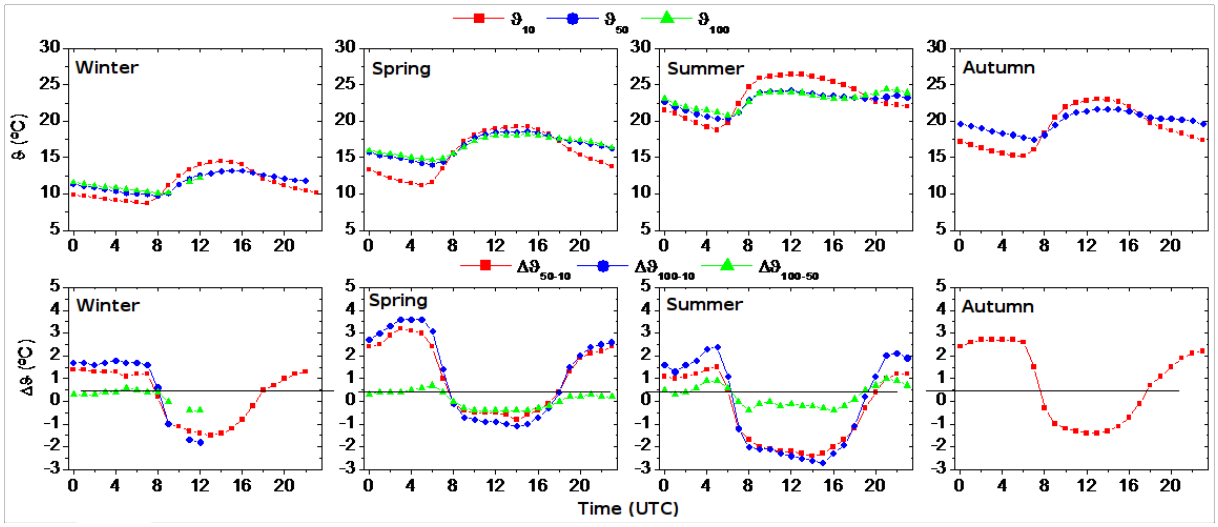

Figure 3. Seasonal evolution of the potential temperature and its difference at 10, 50 and 100 m, according to available data from the hourly values of 2009.

from the SW-W and NW-NE. The development of coastal breeze is also common from May to September (Adame et al., 2010a, 2010b).

From the records in the tower at a height of 100 m, we analyzed the behavior presented by the surface layer in the meteorological scenarios mentioned. All situations observed during the study year, 2009, were analyzed. Two main behavior patterns of the boundary layer were identified. Thus, under coastal breeze conditions or NE synoptic flows there is a surface layer with planetary boundary layer characteristics, i.e. affected by the daytime heating and nighttime cooling of the earth's surface. Meanwhile, under the effect of synoptic flows from the SW-W or NW, the surface layer seems to be affected by the marine boundary layer. As an example, two cases are outlined below, one of coastal breeze and another one of synoptic flow from the SW-W. In order to analyze them, the time evolution of the potential temperature, Bulk Richardson Number and wind (speed and direction) are shown.

3.3.1 Behavior of the surface layer in a coastal breeze scenario: 27 to 31 July 2009

During the last five days of July the weather in the area was ruled by the development of coastal breeze mechanisms. In other words, a daily regime of wind blowing inland from the sea in a direction perpendicular to the coastline (from the W) and a nightly regime in the same direction but in the opposite sense (from the N-NE). Figure 4 shows the wind direction records, which demonstrate that this pattern is similar at all three levels, so flows do not differ in the first 100 m of the atmosphere. The differences in potential temperature and the evolution of the Bulk Richardson Number had a day-night variation attributed to the heating and cooling processes of the earth's surface. The potential temperature showed negative differences (unstably stratified), considering the 10-50 and 10-100 m levels, between 7:00-8:00 and 18:00 UTC, and the evolution of the Bulk Richardson Number had negative values as well (unstably stratified case) in the same time slot. The biggest differences for both parameters were found at the lower level, 10 m, and the two top levels, 50 and 100 m. The daytime breeze developed between 9:00-10:00 and 18:00 UTC. Thus, the starting up of a sea breeze occurred with a delay of about two hours from the start of the earth's surface warming. Meanwhile, the night breeze, after a transition period began to be detected at around midnight, with flows of certain intensity, which decreased as the night progressed.

From the results obtained in the first 100 m, it could be estimated that there are ideal conditions for the formation of a mixed layer for about 9 to 10 hours. The maximum differences in potential temperature found in the upper 100 m are of 2-2.5°C. Therefore, the maximum height reached by the convective layer could be high, but we were not able to exactly determine it from this information. During the rest of the day, approximately 14 hours, the differences both in potential temperature and Bulk Richardson Number were positive, reflecting inversion situations in the first 100 m of the atmosphere. The behavior found under these conditions would be affected by nighttime cooling and daytime heating, as occurs in the planetary boundary layer.

3.3.2 Behavior of the surface layer under Atlantic flow: 6 to 8 October 2009

The Atlantic coastal environment in which the tower is located makes scenarios with ocean flows very common in any season. Figure 5 shows the hourly evolution of the wind, potential temperature differences and Bulk Richardson Number in a scenario of this kind which occurred from 6 to 8 Oc-

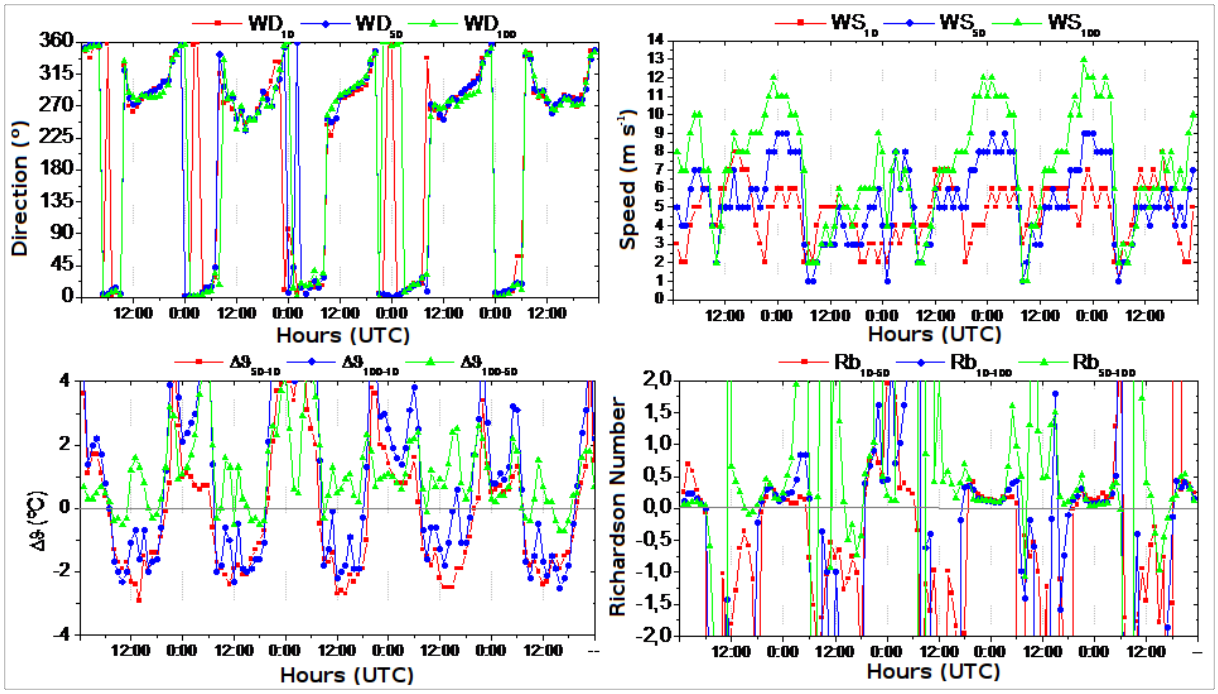

Figure 4. Hourly evolution of the differences of potential temperature, Bulk Richardson Number and wind (speed and direction) at three heights, between 27 and 31 July 2009.

tober 2009. We can see how the wind blew from the SW and rotated to the W and NW. The result was an air mass with a maritime character that swept the study region over these three days.

Although generally synoptic processes showed flows of greater intensity than those of thermal origin, when comparing the speeds measured during this period with the speed presented in the previous section for breeze, we can see how the behavior was reversed. Speeds measured under Atlantic flow are lower than those detected in the breeze development. The reason would be that it is a synoptic situation with an isobaric gradient that is high enough to produce no development of mesoscale processes. However, speeds of moderate intensity, not exceeding 8 m s^{-1}, were registered.

The evolution of potential temperature differences and Bulk Richardson Number in this case do not show clear daily patterns. In the case of potential temperature, differences were negative in a large part of the period, both at day and night; the same result was obtained for the Bulk Richardson Number. Daytime heating and nighttime cooling with a sign change in the differences of the considered parameters were not reflected under such synoptic conditions, nor were the potential temperature differences between levels or the evolution of the Richardson Number. It is possible to indicate that under these conditions the atmospheric surface layer in this coastal environment is influenced by the marine boundary layer, which has more humid air, where heat fluxes do not play an important role, because they do not determine the structure of the boundary layer, and the daily temperature variations on its surface are very small due to the high capacity of the sea to keep warm (Garratt, 1994).

4 Conclusions

This paper presents the first results obtained from the analysis of meteorological records measured at three levels (10, 50 and 100 m) on a 100 m tower at El Arenosillo, southwest IP, in 2009.

In general, temperature variation showed an increasing trend with height, while the relative humidity remained at constant values, or small variations in the first 100 meters. Pressure decreased with height, as expected, and wind speed increased. The analysis of the wind direction at the three levels showed high homogeneity, but a larger northern component was detected at 100 m. Compared to the time series, there was a predominance of winds from NW and SW, caused by cyclonic situations during the warmer months, and little influence from NE flows.

The analysis of the daily seasonal cycles of potential temperature and its differences between the levels throughout the year shows that vertical mixing processes related to unstably stratified stability are longer in summer (12 hours) than in winter (9 hours). It was possible to identify the periods of the day and in every season in which there would be mixing situations (instability) or temperature inversions (stability). However, with the information obtained from potential temperature differences between levels, the height reached both by the mixing layer and the inversion layer can-

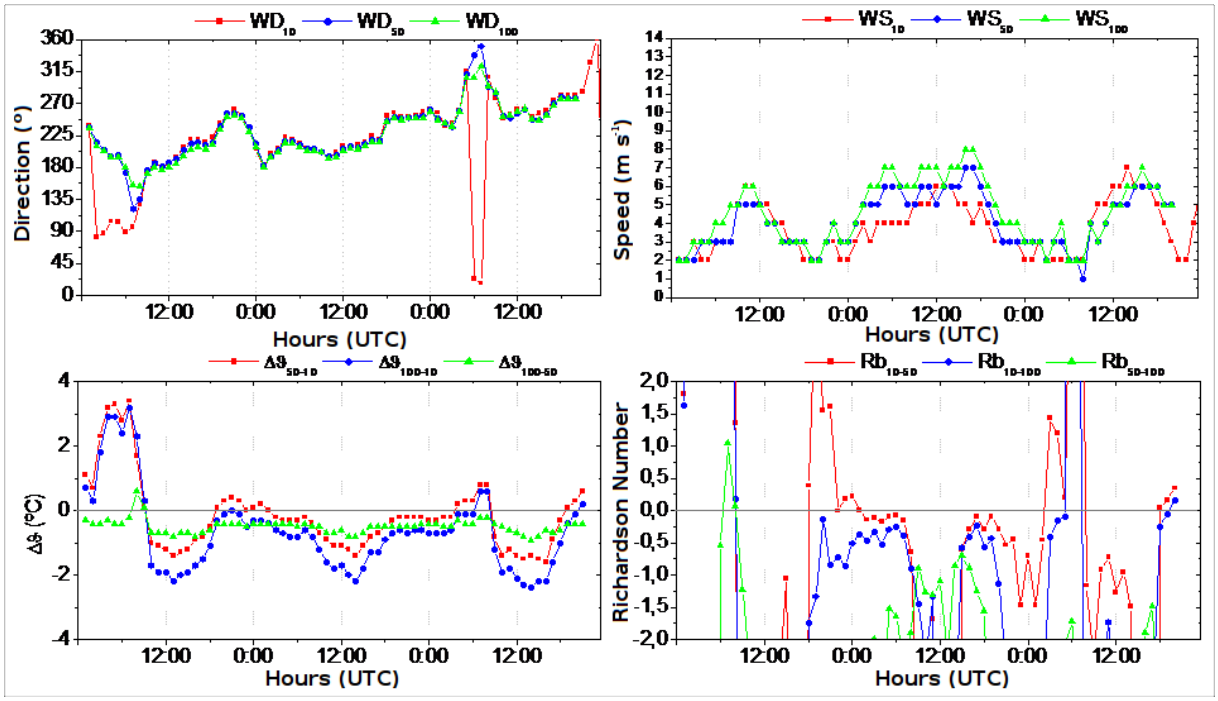

Figure 5. Hourly evolution of the potential temperature differences, Bulk Richardson Number and wind (speed and direction) at three heights, between 6 and 8 October 2009.

not be obtained. In cases of greater intensity of stratification stability, both unstable and stable, the mixed layer and the surface temperature inversion can be above 100 m.

Prevailing weather patterns in the region are well known from previous studies. All scenarios registered during 2009 and the evolution experienced by both the wind (speed and direction) and the potential temperature difference between levels and the Bulk Richardson Number were analyzed. This study has allowed the identification of the existence of two behavior patterns of the surface boundary layer. Thus, in two different weather scenarios, either characterized by the development of the coastal breeze or by the advection of NE flows, they have an atmospheric layer with a similar structure, with a daily pattern very strongly influenced by daytime heating and nighttime cooling. Regarding breezes, a delay between the transitions from breeze regimes to the onset of solar activity was observed, as well as in the formation of the mixed layer. We would point out that the two above-mentioned scenarios present a typical Planetary Boundary Layer structure.

Under SW-W and NW synoptic flow conditions, i.e. in the absence of sea breezes, the latter of the patterns would happen. The differences of potential temperature and Bulk Richardson Number do not present a clear daily cycle, with generally negative values, indicating a possible situation of unstably stratified stability both during the day and at night. These results reflect that in such situations the behavior of the atmospheric boundary layer is characteristic of the marine boundary layer.

References

Adame, J. A., Bolívar, J. P., and De la Morena, B. A., 2010a: *Surface ozone measurements in the southwest of the Iberian Peninsula (Huelva, Spain)*, Environ Sci Pollut Res, **17**, 355–368, doi: 10.1007/s11 356–008–0098–9.

Adame, J. A., Serrano, E., Bolívar, J. P., and De la Morena, B. A., 2010b: *On the Tropospheric Ozone Variations in a Coastal Area of Southwestern Europe under a Mesoscale Circulation*, J Appl Meteor Climatol, **12**, 748–759, doi: 10.1175/2009JAMC2097.1.

Antón, M., Vilaplana, J. M., Kroon, M., Serrano, A., Parias, M., Cancillo, M. L., and De la Morena, B. A., 2010: *The empirically corrected EP-TOMS total ozone data against Brewer measurements at El Arenosillo (Southwestern Spain)*, IEEE Trans Geosci Remote Sensing, **48**, 3039–3045, doi: 10.1109/TGRS.2010.2043 257.

Arya, S. P., 2001: Introduction to micrometeorology, Academy Press, 420 pp.

Crespí, S., 2002: Altura de la capa de mezcla: Caracterización experimental y aplicación de un modelo meteorológico para el estudio de su evolución diurna, Tesis Doctoral, Universidad Complutense de Madrid, 237 pp.

Cuxart, J., Yagüe, C., Morales, G., Terradellas, E., Orbe, J., Calvo, J., Fernández, A., Soler, M. R., Infante, C., Buenestado, P., Espinalt, A., Joergensen, H. E., Rees, J. M., Vilà, J., Redondo, J. M., Cantalapiedra, I. R., and Conangla, L., 2000: *Stable atmospheric boundary layer experiment in Spain (SABLES 98): A report*, Bound Layer Meteor, **96**, 337–370, doi: 10.1023/A:1002609509 707.

Garratt, J. R., 1994: The Atmospheric Boundary Layer, Cambridge University Press, 336 pp.

Grossi, C., Vargas, A., Arnold, D., López-Coto, I., Bolívar, J. P.,

Adame, J. A., and De la Morena, B. A., 2010: Set-up of a Radon Monitoring Station in a 100 m Height Tower in the Southern Coast of Spain, 6th Conference on Protection Against Radon at Home and at Work, Praga (Republica Checa), 13-17/IX/2010, book of Abstracts, 83, ISBN 978-80-01-04603-6.

Grossi, C., Arnold, D., Adame, J. A., López-Coto, I., Bolívar, J. P., De la Morena, B. A., and Vargas, A., 2012: *Atmospheric 222Rn concentration and source term at El Arenosillo 100 m meteorological tower in Southwest Spain*, Radiat Meas, **47**, 149–162, doi:10.1016/j.radmeas.2011.11.006.

Heue, K. P., Brenninkmeijer, C. A. M., Wagner, T., Mies, K., Dix, B., Frieβ, U., Martinsson, B., Slemr, F., and Van Velthoven, P., 2010: *A comparison of DOAS observations by the CARIBIC aircraft and the GOME-2 satellite of the 2008 Kasatochi volcanic SO2 plume*, Atmos Chem Phys Discuss, **10**, 523–558, doi: 10.5194/acpd–10–523–2010.

IPCC, 2007: Intergovermental Panel of Climate Change (IPCC), http://www.ipcc.ch.

Oncley, S. P., Friehe, C. A., Larue, J. C., Businger, J. A., Itsweire, E. C., and Chang, S. S., 1996: *Surface-layer fluxes, profiles, and turbulence measurements over uniform terrain under near-neutral conditions*, J Atmos Sci, **53**, 1029–1044.

Sinha, V., Williams, J., Diesch, J. M., Drewnick, F., Martinez, M., Harder, H., Regelin, E., Kubistin, D., Bozem, H., Hosaynali-Beygi, Z., Fischer, H., Andrés-Hernández, M. D., Kartal, D., Adame, J. A., and Lelieveld, J., 2012: *Constraints on instantaneous ozone production rates and regimes during DOMINO derived using in-situ OH reactivity measurements*, Atmos Chem Phys, **12**, 7269–7283, doi:10.5194/acp–12–7269–2012.

Song, W., Williams, J., Yassaa, N., Martinez, M., Adame, J. A., Hidalgo, P., Bozem, H., and Lelieveld, J., 2011: *Winter and summer characterization of biogenic enantiomeric monoterpenes and anthropogenic BTEX Compounds at a Mediterranean Stone Pine forest site*, J Atmos Chem, **68**, 233–250, doi:10.1007/s10 874–012–9219–4.

Stull, R. B., 1988: An introduction to Boundary layer meteorology, Kluwer Academic Publishers, 666 pp.

Vindel, J. M., Yagüe, C., and Redondo, J. M., 2008: *Structure function analysis and intermittency in the atmospheric boundary layer*, Nonlinear Process Geophys, **15**, 915–929.

Wehner, B., Siebert, H., Ansmann, A., Ditas, F., Siefert, P., Stratmann, F., Wiedensohler, A., Apituley, A., Shaw, R. A., Manninen, H. E., and Kulmala, M., 2010: *Observations of turbulence-induced new particle formation in the residual layer*, Atmos Chem Phys Discuss, **10**, 327–360, doi: 10.5194/acpd–10–327–2010.

Zieger, P., Weingartner, E., Henzing, J., Moerman, M., Leeuw, G. D., Mikkilä, J., Ehn, M., Petäkä, T., Clémer, K., Van Roozendael, M. V., Yilmaz, S., Friess, U., Irie, H., Wagner, T., Shaiganfar, R., Beirle, S., Apituley, A., Wilson, K., and Baltensperger, U., 2010: *Comparison of ambient aerosol extinction coefficients obtained from in-situ, MAX-DOAS and LIDAR measurements at Cabauw*, Atmos Chem Phys Discuss, **10**, 29 683–29 734, doi: 10.5194/acpd–10–29 683–2010.